CAMBRIDGE
UNIVERSITY PRESS

Article

Mauriziodiniite, NH$_4$(As$_2$O$_3$)$_2$I, the ammonium and iodine analogue of lucabindiite from the Torrecillas mine, Iquique Province, Chile

Anthony R. Kampf[1]* [iD], Barbara P. Nash[2] and Arturo A. Molina Donoso[3]

[1]Mineral Sciences Department, Natural History Museum of Los Angeles County, 900 Exposition Boulevard, Los Angeles, CA 90007, USA; [2]Department of Geology and Geophysics, University of Utah, Salt Lake City, Utah 84112, USA; and [3]Los Algarrobos 2986, Iquique, Chile

Abstract

The new mineral mauriziodiniite (IMA2019-036), NH$_4$(As$_2$O$_3$)$_2$I, was found at the Torrecillas mine, Iquique Province, Chile, where it is a secondary alteration phase associated with calcite, cuatrocapaite-(NH$_4$), lavendulan, magnesiokoritnigite and torrecillasite on matrix consisting of native arsenic, arsenolite and pyrite. Mauriziodiniite occurs as hexagonal tablets up to $\sim$300 μm in diameter. Crystals are colourless and transparent, with pearly to adamantine lustre and white streak. The Mohs hardness is $\sim$1. Tablets are sectile and easily flexible, but not elastic. Fracture is curved, irregular and stepped. Cleavage is perfect on {001}. The calculated density is 3.916 g/cm^3. Optically, mauriziodiniite is uniaxial (–) with ω = 2.07(calc) and ε = 1.770(5) (white light). The empirical formula, determined from electron microprobe analyses, is (NH$_4$)$_{0.94}$K$_{0.03}$(As$_2$O$_3$)$_2$I$_{0.92}$Cl$_{0.03}$. Mauriziodiniite is hexagonal, $P6/mmm$, a = 5.289(2), c = 9.317(2) Å, V = 225.68(18) Å^3 and Z = 1. The structure, refined to R_1 = 4.16% for 135 I_o > 2σI reflections, contains three types of layers: (1) a planar neutral As$_2$O$_3$ (arsenite) sheet; (2) an NH$_4^+$ layer that links adjacent arsenite sheets *via* bonds to their O atoms; and (3) an I$^-$ layer that links adjacent arsenite sheets *via* bonds to their As atoms. The layer sequence is I–As$_2$O$_3$–NH$_4$–As$_2$O$_3$–I. Mauriziodiniite is isostructural with lucabindiite and is structurally related to gajardoite, cuatrocapaite-(NH$_4$), cuatrocapaite-(K) and torrecillasite.

Introduction

Our studies on the secondary mineralisation at the small, long-inactive Torrecillas mine, in the northern Atacama Desert of Chile, have thus far yielded a remarkable array of new mineral species, the majority of which are arsenic oxysalts. These include twelve new hydrogen arsenates and four new arsenites (see Kampf *et al*., 2019*a*). The new mineral species mauriziodiniite, described herein, is the fifth new arsenite to be discovered at Torrecillas. Mauriziodiniite, NH$_4$(As$_2$O$_3$)$_2$I, is the ammonium and iodine analogue of lucabindiite, K(As$_2$O$_3$)$_2$Cl. Another potentially new arsenite, the ammonium analogue of lucabindiite, with the ideal formula NH$_4$(As$_2$O$_3$)$_2$Cl, is currently under study.

The name mauriziodiniite honours Maurizio Dini of La Serena, Chile (born 1968). Mr. Dini is an Italian amateur mineralogist who has lived in Chile since 1998. He is a Professor of Sociology at both Universidad Pedro de Valdivia and Universidad Central de Chile. Since 2002, he has collaborated with Chilean geologist Arturo Molina, whom he considers his geological and mineralogical mentor and with whom he has discovered many new minerals. Mr. Dini's principal mineralogical interests are sulfides and sulfosalts of Ag, Sb and As, and secondary minerals, especially arsenites and arsenates. He was involved in the discovery of santarosaite, juangodoyite and sanrománite at the Santa Rosa silver mine (Iquique Province, Chile) and, more recently, in the discovery of the unique secondary arsenic-rich secondary mineral assemblages at Torrecillas. He is a co-author of numerous new mineral descriptions including alcaparrosaite, bariopharmacoalumite, camaronesite, camanchacaite, canutite, chongite, cuatrocapaite-(NH$_4$), cuatrocapaite-(K), currierite, erazoite, gajardoite, joteite, juansilvaite, leverettite, magnesiocanutite, magnesiofluckite, magnesiokoritnigite, mendozavilite-KCa, obradovicite-NaNa, paratacamite-(Mg), picaite, ríosecoite, shilovite, tapiaite, tondiite and torrecillasite (See Pasero, 2020 and references therein). Maurizio Dini and one of the authors (AAMD) collected mauriziodiniite; Mr. Dini recognised it as a potentially new mineral and provided the holotype specimen. He has given permission for the mineral to be named in his honour. Note that the compound name mauriziodiniite is proposed because of the similarity of 'diniite' to the existing mineral named dinite. Also, note that mauriziodiniite is an analogue of another mineral with a compound name – lucabindiite. Furthermore, quite serendipitously, the compound name includes the letter sequence 'iodin'.

The new mineral and the name have been approved by the International Mineralogical Association (IMA2019-036, Kampf

et al., 2019c). The description is based upon one holotype specimen deposited in the collections of the Natural History Museum of Los Angeles County, 900 Exposition Boulevard, Los Angeles, CA 90007, USA, catalogue number 67365.

Occurrence

The new mineral was found on one specimen at the Torrecillas mine, Salar Grande, Iquique Province, Tarapacá Region, Chile (~20°58'13''S, 70°8'17''W). Torrecillas Hill, on which the Torrecillas mine is located, is composed of four different rock units. The Coastal Range Batholith (mainly gabbros) extends from the seashore to the Pan-American Road along the base of Torrecillas Hill. At the foot of Torrecillas Hill is a small area of contact metamorphic rocks in which garnet crystals occur in metamorphosed shales. Higher on the hill, the rocks are predominantly porphyritic andesitic lavas of the Jurassic La Negra Formation (García, 1967; Buchelt and Tellez, 1988). The Torrecillas deposit, in which the new minerals were found, consists of two main veins rich in secondary arsenic and copper minerals that intersect metamorphosed marine shales and lavas. These mineralised veins are genetically related to the aforementioned porphyritic andesitic lavas. More information on the geology and mineralogy of the area is provided by Gutiérrez (1975).

The rare secondary chlorides, arsenates and arsenites (and associated sulfates) have been found at three main sites on the hill: an upper pit measuring ~8 m long and 3 m deep, a lower pit ~100 m from the upper pit and measuring ~5 m long and 3 m deep, and a mine shaft adjacent to the lower pit and lower on the hill. Mauriziodiniite was found in a recent excavation a few metres above the shaft.

Mauriziodiniite is a secondary alteration phase occurring on matrix consisting of native arsenic, arsenolite and pyrite in association with calcite, cuatrocapaite-(NH4) (Kampf *et al.*, 2019b), lavendulan, magnesiokoritnigite (Kampf *et al.*, 2013) and torrecillasite (Kampf *et al.*, 2014). The secondary assemblages at the Torrecillas deposit are interpreted as principally having formed from the oxidation of native arsenic and other As-bearing primary phases, followed by later alteration by saline fluids derived from evaporating meteoric water under hyperarid conditions (*cf.* Cameron *et al.*, 2007); however, considering the proximity of the Torrecillas deposit to the Pacific Ocean, it seems possible that the frequent dense coastal *camanchaca* fogs have also played a role in the alteration of the veins and the formation of the secondary minerals, particularly in the recent past, since the exhumation of the deposit well above sea level on Torrecillas Hill (see Kampf *et al.*, 2019a).

Physical and optical properties

Mauriziodiniite occurs as hexagonal tablets with bevelled edges, exhibiting the forms {100}, {101} and {001} (Fig. 1). Tablets are up to 0.3 mm in diameter and grow in irregular clusters (Fig. 2). No twinning was observed. Crystals are transparent, with pearly to adamantine lustre and white streak. The mineral does not fluoresce in longwave or shortwave ultraviolet light. The Mohs hardness is ~1 based on scratch tests. The tenacity is sectile and tablets are flexible, but not elastic. Cleavage is perfect on {001}. The sectile tenacity and perfect cleavage contribute to a fracture with curved, irregular and stepped characteristics. The density was not measured because of the paucity of material and the difficulty of observing the small crystals in Clerici solution. The calculated density is
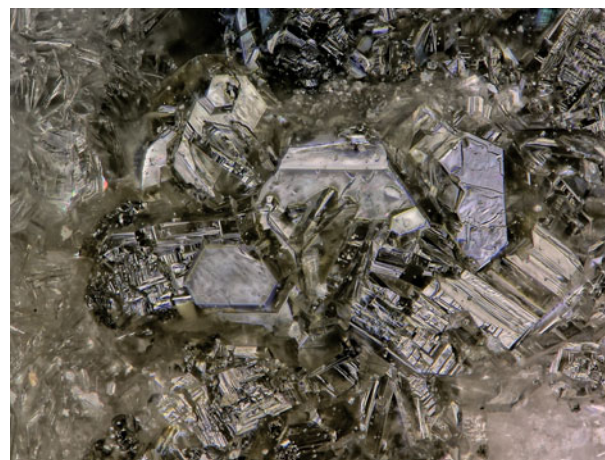

Fig. 1. Mauriziodiniite tablets on cuatrocapaite-(NH4); field of view = 0.84 mm across, holotype specimen #67365.
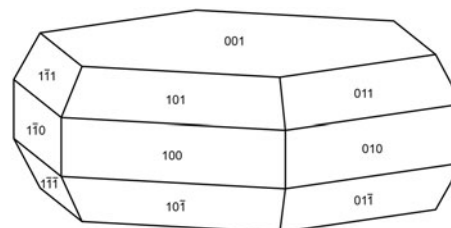

Fig. 2. Crystal drawing of mauriziodiniite; clinographic projection.

3.916 g/cm^3 for the empirical formula and 3.977 g/cm^3 for the ideal formula. The mineral is insoluble at room temperature in concentrated HCl or concentrated H_2SO_4.

Optically, mauriziodiniite is uniaxial (–) with $\varepsilon = 1.770(5)$ (measured in white light). ω is significantly greater than 2.00 based upon measurement in 2.00 index liquid. Because liquids of higher index were not available, direct measurement of ω was not possible. Measurement of the $\omega - \varepsilon$ birefringence using a Berek compensator provided an approximate value of 0.30, which allows the calculation of ω as 2.07. The mineral is nonpleochroic.

Raman spectroscopy

Raman spectroscopy was done on a Horiba XploRa+ micro-Raman spectrometer using an incident wavelength of 532 nm at 50% power, laser slit of 50 μm, 1800 gr/mm diffraction grating and a 100x (0.9 NA) objective. In addition to mauriziodiniite, spectra were recorded from 4000 to 60 cm^{-1} for gajardoite, $KCa_{0.5}(As_2^{3+}O_3)_2Cl_2 \cdot 5H_2O$, cuatrocapaite-(NH4), $(NH_4,K)_3(NaMg\square)$ $(As_2^{3+}O_3)_6Cl_6 \cdot 16H_2O$, and a potentially new phase that corresponds to the NH4 analogue of lucabindiite (with some enrichment in I), $(NH_4,K)(As_2O_3)_2(Cl,I)$ [henceforth referred to as 'lucabindiite-(NH4)']. In all cases, the laser was oriented perpendicular to the plates. The aforementioned phases all occur in the same general assemblage at Torrecillas, all occur as colourless hexagonal plates, and all have structures containing identical planar neutral As_2O_3 (arsenite) sheets that are included in the same layer sequences: $(Cl,I)-As_2O_3-(K,NH_4)-As_2O_3-(Cl,I)$. The structures of gajardoite and cuatrocapaite differ from that of mauriziodiniite and 'lucabindiite-(NH4)' in that they each contain an additional layer consisting of cations and H_2O.
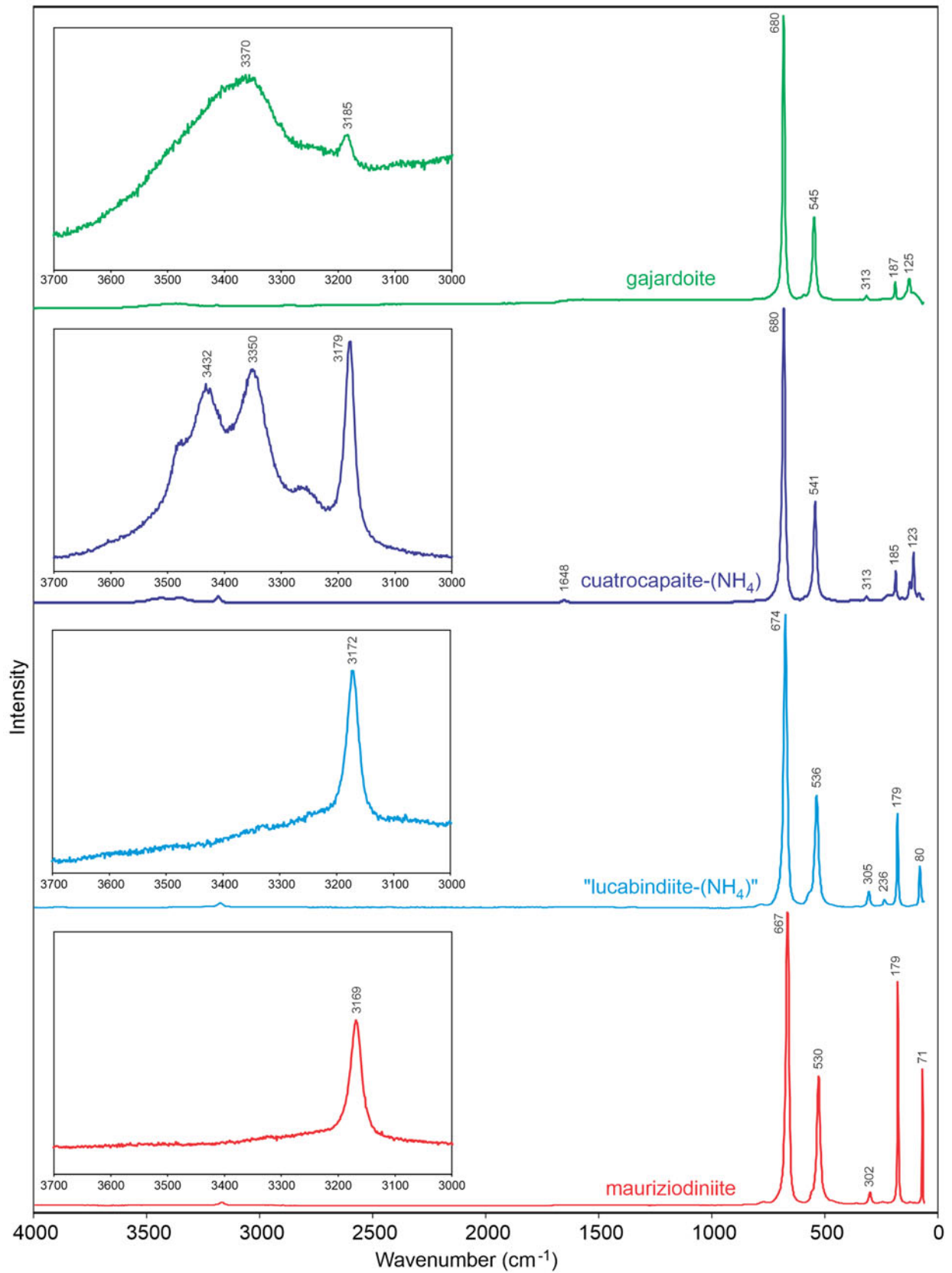
Fig. 3. Raman spectra of gajardoite, cuatrocapaite-(NH$_4$), I-rich 'lucabindiite-(NH$_4$)' and mauriziodiniite.

Table 1. Compositional data (in wt.%) for mauriziodiniite.

Constituent	Mean	Range	S.D.	Probe standard
$(NH_4)_2O$	4.43	4.15–4.81	0.34	Cr_2N
K_2O	0.29	0.27–0.31	0.02	Sanidine
As_2O_3	71.83	71.04–72.60	0.78	GaAs
I	21.27	21.04–21.60	0.30	TlBrI
Cl	0.22	0.17–0.31	0.08	Tugtupite
O=(I + Cl)	−1.39			
Total	96.65			

S.D. – standard deviation.

Table 2. Powder X-ray data (*d* in Å) for mauriziodiniite.

I_{obs}	I_{calc}	d_{obs}	d_{calc}	*h k l*
29	**39**	**9.35**	**9.3170**	**0 0 1**
19	**21**	**4.644**	**4.6585**	**0 0 2**
	4		4.5804	1 0 0
11	13	4.113	4.1105	1 0 1
100	**100**	**3.269**	**3.2661**	**1 0 2**
71	**54**	**2.644**	**2.6445**	**1 1 0**
42	**19, 22**	**2.554**	**2.5705, 2.5440**	**1 0 3, 1 1 1**
4	7	2.328	2.3293	0 0 4
7	6	2.300	2.2998	1 1 2
	1		2.2902	2 0 0
	1		2.0762	1 0 4
12	13	2.0557	2.0553	2 0 2
5	5	2.0099	2.0134	1 1 3
	4		1.8634	0 0 5
20	**20**	**1.8460**	**1.8432**	**2 0 3**
14	17	1.7486	1.7479	1 1 4
	1		1.7312	2 1 0
2	2	1.7030	1.7021	2 1 1
27	**24**	**1.6232**	**1.6228**	**2 1 2**
	1		1.5528	0 0 6
36	**10, 22**	**1.5241**	**1.5268, 1.5232**	**3 0 0, 1 1 5**
11	8,5	1.5101	1.5122, 1.5067	2 1 3, 3 0 1
2	2	1.4748	1.4706	1 0 6
3	2,1	1.4500	1.4509, 1.4454	3 0 2, 2 0 5
	1		1.3702	3 0 3
	1		1.3390	1 1 6
10	10	1.3217	1.3223	2 2 0
	2		1.3091	2 2 1

The strongest lines are given in bold.

The four spectra exhibit many similarities (Fig. 3). Two of the most prominent bands in all four spectra are at 680–667 cm^{-1} and 545–530 cm^{-1}, which can be assigned to $As^{3+}O_3$ stretching and bending, respectively. It should be noted that the Raman modes associated with arsenite groups vary considerably depending upon their As–O–As linkages (*cf.* Szymanski *et al.*, 1968; Bahfenne and Frost, 2010). We were unable to find any past Raman studies on compounds containing hexagonal As_2O_3 sheets similar to those occurring in the structures of these four minerals; however, the aforementioned band assignments seem generally consistent with earlier studies.

In the 3700–3000 cm^{-1} region (expanded insets in Fig. 3), both gajardoite and cuatrocapaite-(NH_4) show prominent broad bands corresponding to O–H stretching, which are absent in the spectra of mauriziodiniite and 'lucabindiite-(NH_4)'; however, all four spectra exhibit a relatively sharp band in the range 3185–3169 cm^{-1}. This band can be assigned to N–H stretching associated with the NH_4^+ units (*cf.* Mairesse *et al.*, 1978). The band is only weakly displayed in the gajardoite spectrum; however, this is an indication that a small amount of NH_4 is present in

Table 3. Data collection and structure refinement details for mauriziodiniite.

Crystal data	
Structural formula*	$[(NH_4)_{0.97}K_{0.03}]_{\Sigma 1}(As_2O_3)_2(I_{0.95}Cl_{0.05})_{\Sigma 1}$
Crystal size (μm)	100 × 70 × 15
Crystal system, space group	Hexagonal, $P6/mmm$ (#191)
Temperature (K)	293(2)
Unit-cell dimensions (Å)	$a = 5.289(2)$, $c = 9.317(2)$
V (Å³)	225.68(18)
Z	1
Density (g/cm³)	3.920
Absorption coefficient (mm^{-1})	17.947
Data collection	
Diffractometer	Rigaku R-Axis Rapid II
X-ray radiation	Mo$K\alpha$ ($\lambda = 0.71075$ Å)
$F(000)$	238.6
θ range (°)	4.38 to 27.27
Reflections collected/unique	1410/139; $R_{int} = 0.053$
Reflections with $I_o > 2\sigma I$	135
Index ranges	$-6 \leq h \leq 6$, $-6 \leq k \leq 6$, $-12 \leq l \leq 12$
Refinement	
Refinement method	Full-matrix least-squares on F^2
Completeness to θ = 27.27°	99.3%
Parameters/restraints	13/0
GoF	1.156
Final R indices [$I_o > 2\sigma I$]	$R_1 = 0.0441$, $wR_2 = 0.1173$
R indices (all data)	$R_1 = 0.0446$, $wR_2 = 0.1179$
Largest diff. peak/hole (e^-/A^3)	+2.85/−0.92

* The structure refinement did not include H sites.
$R_{int} = \Sigma|F_o^2 - F_o^2(\text{mean})|/\Sigma[F_o^2]$. GoF = $S = \{\Sigma[w(F_o^2 - F_c^2)^2]/(n-p)\}^{1/2}$. $R_1 = \Sigma||F_o| - |F_c||/\Sigma|F_o|$. $wR_2 = \{\Sigma[w(F_o^2 - F_c^2)^2]/\Sigma[w(F_o^2)^2]\}^{1/2}$; $w = 1/[\sigma^2(F_o^2) + (aP)^2 + bP]$ where a is 0.073, b is 2.3342 and P is $[2F_c^2 + \text{Max}(F_o^2, 0)]/3$.

this mineral, presumably accommodated in the partially occupied K site in the structure, even though it was not reported in the original chemical analyses (Kampf *et al.*, 2016).

Composition

Analyses (3 points) were performed at the University of Utah on a Cameca SX-50 electron microprobe with four wavelength dispersive spectrometers and using *Probe for EPMA* software. Analytical conditions were 15 keV accelerating voltage, 20 nA beam current and a beam diameter of 15 μm. Raw X-ray intensities were corrected for matrix effects with a φρ(z) algorithm (Pouchou and Pichoir, 1991). No other elements were detected by EDS or by WDS wavescans. There was minor damage from the electron beam. The analytical results are provided in Table 1. Loss of volatiles (NH_4, Cl and I), perhaps associated with the minor beam damage, could account for the low analytical total.

The empirical formula based on 4 As atoms per formula unit is $(NH_4)_{0.94}K_{0.03}(As_2O_3)_2I_{0.92}Cl_{0.03}$. The simplified structural formula is $(NH_4,K)(As_2O_3)_2(I,Cl)$ and the idealised formula is $NH_4(As_2O_3)_2I$, which requires $(NH_4)_2O$ 4.82, As_2O_3 73.19, I 23.47, O = I −1.48, total 100.00 wt.%. The Gladstone-Dale compatibility $1 - (K_P/K_C)$ for the empirical formula is −0.013 and for the ideal formula is 0.004, both in the range of superior compatibility (Mandarino, 2007).

X-ray crystallography and structure refinement

Both powder and single-crystal X-ray studies were carried out using a Rigaku R-Axis Rapid II curved imaging plate microdiffractometer, with monochromatic Mo$K\alpha$ radiation. For the powder-diffraction study, a Gandolfi-like motion on the φ and ω axes was used to randomise the sample, and observed *d* values

Table 4. Atom coordinates and displacement parameters (Å^2) for mauriziodiniite.

	x/a	y/b	z/c	Occupancy	U_{eq}	U^{11}	U^{22}	U^{33}	U^{23}	U^{13}	U^{12}
N(NH$_4$)	0	0	½	(NH$_4$)$_{0.97}$K$_{0.03}$	0.039(7)	0.046(12)	0.046(12)	0.025(14)	0	0	0.023(6)
As	⅓	⅔	0.78950(16)	As	0.0124(6)	0.0077(7)	0.0077(7)	0.0218(10)	0	0	0.0039(3)
O	½	0	0.6859(9)	O	0.0148(14)	0.011(3)	0.007(4)	0.025(4)	0	0	0.0034(18)
I	0	0	0	I$_{0.953}$Cl$_{0.047(15)}$	0.0207(8)	0.0152(9)	0.0152(9)	0.0317(14)	0	0	0.0076(5)

Table 5. Selected bond distances (Å) for mauriziodiniite.

N(NH$_4$)–O (×12)	3.161(5)
As–O (×3)	1.806(4)
As–I (×3)	3.6290(13)

Table 6. Bond-valence analysis for mauriziodiniite. Values are expressed in valence units (vu).

	O	I	Σ_c
NH$_4$	×2↓ 0.08 ×12→		0.96
As	×2↓ 0.93 ×3→	×12↓ 0.06 ×3→	2.97
Σ_a	2.02	0.72	

Multiplicities indicated by ×↓→; bond strengths based upon site occupancies; K$^+$–O and As^{3+}–O bond-valence parameters are from Gagné and Hawthorne (2015), NH^{4+}–O are from Garcia-Rodriguez *et al.* (2000), As^{3+}–Cl are from Brese and O'Keeffe (1991) and As^{3+}–I are from I.D. Brown (private communication).

Fig. 4. Arsenite sheet viewed along **c** in the structures of mauriziodiniite, lucabindiite, gajardoite and cuatrocapaite-(NH$_4$). The As atoms are red and the O atoms are white.

and intensities were derived by profile fitting using *JADE 2010* software (Materials Data, Inc.). The powder data presented in Table 2 show good agreement with the pattern calculated from the structure determination. Unit-cell parameters refined from the powder data using *JADE 2010* with whole pattern fitting are $a = 5.2832(10)$, $c = 9.3094(19)$ Å and $V = 225.03(10)$ Å^3.

The Rigaku *CrystalClear* software package was used for processing the structure data, including the application of an empirical absorption correction using the multi-scan method with *ABSCOR* (Higashi, 2001). The structure was solved by the charge-flipping method using *SHELXT* (Sheldrick, 2015a). The atom coordinates were then transformed to correspond to those of synthetic NH$_4$(As$_2$O$_3$)$_2$I (Pertlik, 1988), with which mauriziodiniite is isostructural. Refinement proceeded by full-matrix least-squares on F^2 using *SHELXL-2016* (Sheldrick, 2015b). The NH$_4$ site was refined with joint occupancy by N and K and the I site was refined with joint occupancy by I and Cl providing the formula [(NH$_4$)$_{0.65}$K$_{0.35}$)](As$_2$O$_3$)$_2$(I$_{0.94}$Cl$_{0.06}$); however, the resulting U_{eq} for the NH$_4$ site of 0.088(11) suggested a lower K and higher N content. Consequently, the site was instead assigned an occupancy of N$_{0.97}$K$_{0.03}$, more consistent with the EPMA. This resulted in a more reasonable U_{eq} for the NH$_4$ site of 0.039(7). The difference Fourier revealed one possible H site at (0, 0, 0.424), 0.71 Å from the N site along the 6-fold axis; however, no other possible H sites were found and no H sites were included in the final refinement. The data collection and refinement details are given in Table 3, atom coordinates and displacement parameters in Table 4, selected bond distances in Table 5 and bond-valence sums in Table 6. The crystallographic information files have been deposited with the Principal Editor of *Mineralogical Magazine* and are available as Supplementary material (see below).
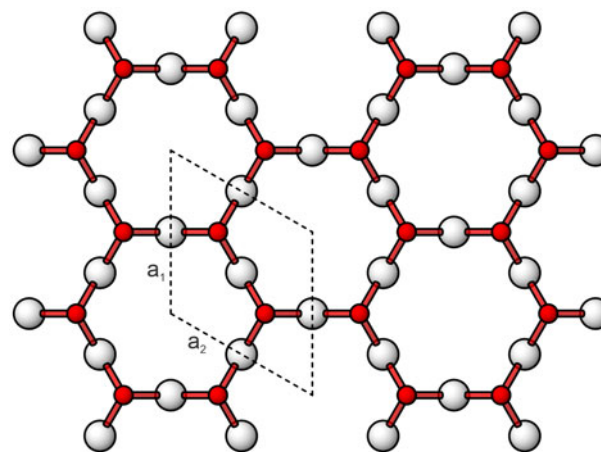
Description of the structure

Mauriziodiniite is isostructural with lucabindiite, (K,NH$_4$)(As$_2$O$_3$)$_2$(Cl,Br) (Garavelli *et al.*, 2013), and with a series of (K,NH$_4$)(As$_2$O$_3$)$_2$(Cl,Br,I) synthetics reported by Pertlik (1988). The structure (Fig. 4) contains three types of layers: (1) a planar neutral As$_2$O$_3$ (arsenite) sheet with hexagonal symmetry (Fig. 4); (2) an NH$_4^+$ layer that links adjacent arsenite sheets *via* bonds to their O atoms; and (3) an I$^-$ layer that links adjacent arsenite sheets *via* bonds to their As atoms. The layer sequence is I–As$_2$O$_3$–NH$_4$–As$_2$O$_3$–I. The bond-valence sum for the I site (0.74 valence units) is somewhat low; however, it is much higher than those observed for Cl in the lucabindiite (0.31 vu) and gajardoite (0.24 vu) structures. This phenomenon is probably caused by the repulsive effect of the lone electron pair of the As^{3+}.

Gajardoite [(K,NH$_4$)Ca$_{0.5}$(As$_2$O$_3$)$_2$Cl$_2$·5H$_2$O; Kampf *et al.*, 2016] and the series cuatrocapaite-(NH$_4$)–cuatrocapaite-(K) [(NH$_4$,K)$_3$(NaMg□)(As$_2$O$_3$)$_6$Cl$_6$·16H$_2$O; Kampf *et al.*, 2019b] have structures with Cl–As$_2$O$_3$–(K,NH$_4$)–As$_2$O$_3$–Cl layer sequences that are topologically equivalent to those in lucabindiite and mauriziodiniite; however, the gajardoite and cuatrocapaite structures both incorporate an additional layer. Gajardoite incorporates a disordered Ca–H$_2$O layer and the cuatrocapaite series incorporates a disordered Na–Mg–H$_2$O layer. The structures of mauriziodiniite, gajardoite and cuatrocapaite-(NH$_4$) are compared in Fig. 5. Torrecillasite [Na(As$_2$O$_3$)$_2$Cl; Kampf *et al.*, 2014] also has a layer structure, with the sequence Cl–As$_2$O$_3$–Na–As$_2$O$_3$–Cl; however, the As$_2$O$_3$ layer in torrecillasite is geometrically and topologically different from that in the other minerals.
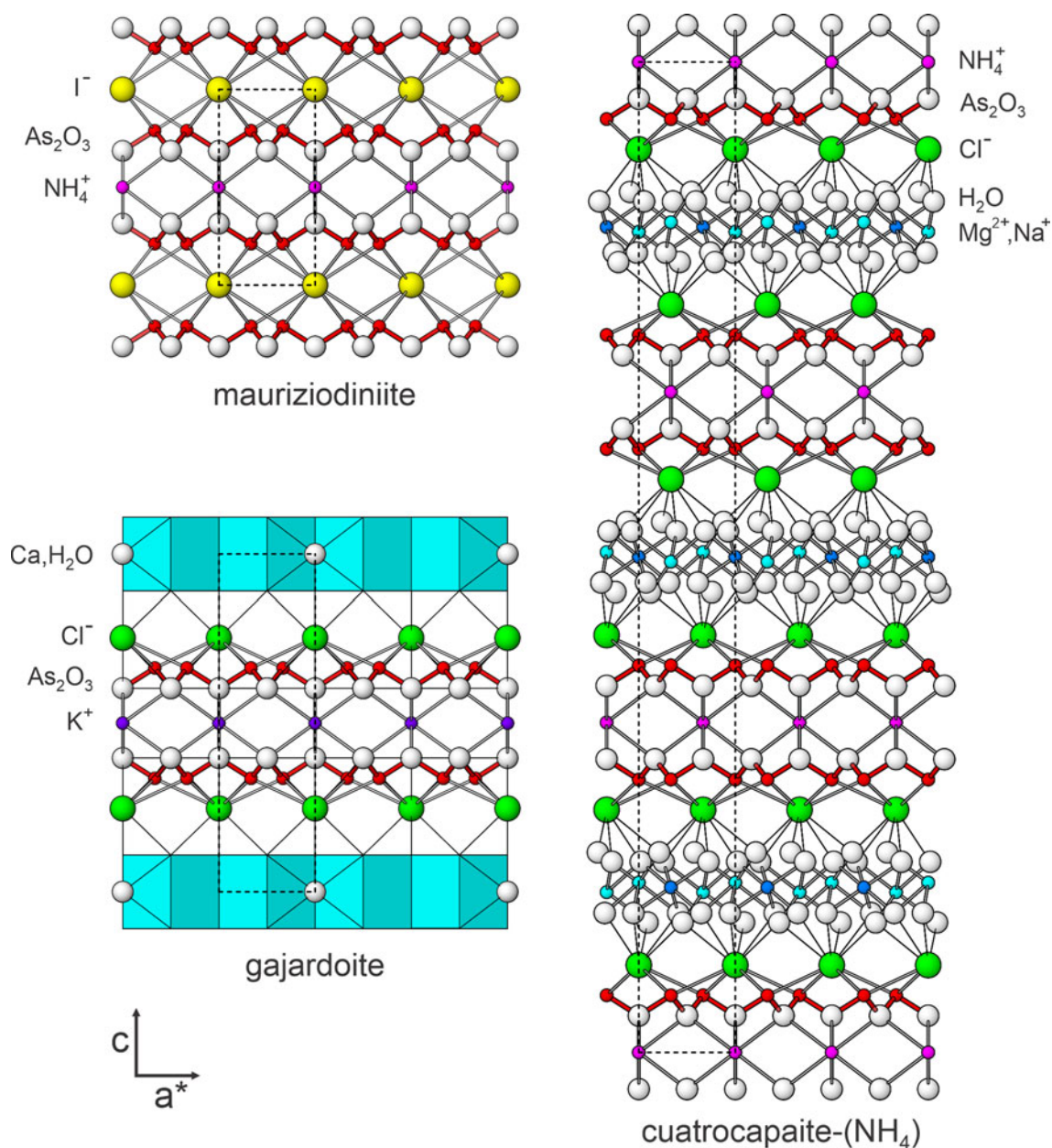
Fig. 5. The structures of mauriziodiniite, gajardoite and cuatrocapaite-(NH₄).

References

Bahfenne S. and Frost R.L. (2010) A review of the vibrational spectroscopic studies of arsenite, antimonite, and antimonate minerals. *Applied Spectroscopy Reviews*, **45**, 101–129.

Brese N.E. and O'Keeffe M. (1991) Bond-valence parameters for solids. *Acta Crystallographica*, **B47**, 192–197.

Buchelt M. and Tellez C. (1988) The Jurassic La Negra Formation in the area of Antofagasta, north Chile (lithology, petrography, geochemistry). Pp. 171–182 in: *The Southern Central Andes* (H. Bahlburg, C. Breitkreuz and P. Giese, editors). Lecture Notes in Earth Sciences 17. Springer, Berlin–Heidelberg–New York.

Cameron E.M., Leybourne M.I. and Palacios C. (2007) Atacamite in the oxide zone of copper deposits in northern Chile: involvement of deep formation waters? *Mineralium Deposita*, **42**, 205–218.

Gagné O.C. and Hawthorne F.C. (2015) Comprehensive derivation of bond-valence parameters for ion pairs involving oxygen. *Acta Crystallographica*, **B71**, 562–578.

Garavelli A., Mitolo D., Pinto D. and Vurro F. (2013) Lucabindiite, (K,NH₄) As₄O₆(Cl,Br), a new fumarole mineral from the "La Fossa" crater at Vulcano, Aeolian Islands, Italy. *American Mineralogist*, **98**, 470–477.

García F. (1967) Geologia del Norte Grande de Chile. *Simposio Geosinclinal Andino, Sociedad Geológica de Chile Publicaciones*, **3**, 138 pp.

García-Rodríguez L., Rute-Pérez Á., Piñero J.R., and González-Silgo C. (2000) Bond-valence parameters for ammonium-anion interactions. *Acta Crystallographica*, **B56**, 565–569.

Gutiérrez H. (1975) *Informe Sobre una Rápida Visita a la Mina de Arsénico Nativo, Torrecillas*. Instituto de Investigaciones Geológicas, Iquique, Chile.

Higashi T. (2001) *ABSCOR*. Rigaku Corporation, Tokyo.

Kampf A.R., Nash B.P., Dini M. and Molina Donoso A.A. (2013) Magnesiokoritnigite, $Mg(AsO_3OH)·H_2O$, from the Torrecillas mine, Iquique Province, Chile: the Mg-analogue of koritnigite. *Mineralogical Magazine*, **77**, 3081–3092.

Kampf A.R., Nash B.P., Dini M. and Molina Donoso A.A. (2014) Torrecillasite, $Na(As,Sb)_4^{3+}O_6Cl$, a new mineral from the Torrecillas mine, Iquique Province, Chile: description and crystal structure. *Mineralogical Magazine*, **78**, 747–755.

Kampf A.R., Nash B.P., Dini M. and Molina Donoso A.A. (2016) Gajardoite, $KCa_{0.5}As_4^{3+}O_6Cl_2·5H_2O$, a new mineral related to lucabindiite and torrecillasite from the Torrecillas mine, Iquique Province, Chile. *Mineralogical Magazine*, **80**, 1265–1272.

Kampf A.R., Nash B.P., Dini M. and Molina Donoso A.A. (2019a) Camanchacaite, chinchorroite, espadaite, magnesiofluckite, picaite and ríosecoite: six new hydrogen-arsenate minerals from the Torrecillas mine, Iquique Province, Chile. *Mineralogical Magazine*, **83**, 655–671.

Kampf A.R., Chukanov N.V., Möhn G., Dini M., Molina Donoso A.A. and Friis H. (2019b) Cuatrocapaite-(NH_4) and cuatrocapaite-(K), two new minerals from the Torrecillas mine, Iquique Province, Chile, related to lucabindiite and gajardoite. *Mineralogical Magazine*, **83**, 741–748

Kampf A.R., Nash B.P. and Molina Donoso A.A. (2019c) Mauriziodiniite, IMA 2019-036. CNMNC Newsletter, No. 51; *Mineralogical Magazine*, **83**, doi: 10.1180/mgm.2019.58

Mairesse G., Barbier P., Wignacourt J.P., Rubbens A. and Wallart F. (1978). X-Ray, Raman, infrared, and nuclear magnetic resonance studies of the crystal structure of ammonium tetrachloroaluminate, NH_4AlCl_4. *Canadian Journal of Chemistry*, **56**, 764–771.

Mandarino J.A. (2007) The Gladstone–Dale compatibility of minerals and its use in selecting mineral species for further study. *The Canadian Mineralogist*, **45**, 1307–1324.

Pasero M. (2020) *The New IMA List of Minerals*. http://cnmnc.main.jp/

Pertlik F. (1988) The compounds KAs_4O_6X (X = Cl, Br, I) and $NH_4As_4O_6X$ (X = Br, I): hydrothermal syntheses and structure determinations. *Monatshefte für Chemie*, **119**, 451–456.

Pouchou J.-L. and Pichoir F. (1991) Quantitative analysis of homogeneous or stratified microvolumes applying the model "PAP". Pp. 31–75 in: *Electron Probe Quantification* (K.F.J. Heinrich and D.E. Newbury, editors). Plenum Press, New York.

Sheldrick G.M. (2015a) SHELXT – Integrated space-group and crystal-structure determination. *Acta Crystallographica*, **A71**, 3–8.

Sheldrick G.M. (2015b) Crystal Structure refinement with *SHELX*. *Acta Crystallographica*, **C71**, 3–8.

Szymanski H.A., Marabella L., Hoke J. and Harter J. (1968) Infrared and Raman studies of arsenic compounds. *Applied Spectroscopy*, **22**, 297–304.